

## Birefringence of amorphous polyarylates: 2. Dynamic measurement on a polyarylate with low optical anisotropy

Tadashi Inoue\*, Eui-Jeong Hwang and Kunihiro Osaki

*Institute for Chemical Research, Kyoto University, Uji, Kyoto 611, Japan*  
 (Received 28 February 1996; revised 15 April 1996)

The complex strain–optical ratio and the complex Young’s modulus of a polyarylate with a low molecular anisotropy, PAr1, were measured around the glass-to-rubber transition zone. The polyarylate was synthesized from 2,2′-dicarboxy biphenyl and 4,4′-dioxydiphenyl-2,2′-propane. The data were analysed with a modified stress–optical rule: The Young’s modulus and the complex strain–optical ratio were separated into two component functions (denoted by G and R) for which the ordinary stress-optical rule held well individually. A comparison of the component functions was made with a conventional amorphous polyarylate (UP) and bisphenol A polycarbonate (PC). The limiting modulus of the R component at high frequencies for PAr1 was about two times higher than that for UP and PC. This result suggested that PAr1 had a highly flexible main-chain structure. This high flexibility was in accord with a zigzag structure of 2,2′-dicarboxy biphenyl unit of the main chain. The stress–optical coefficient for the R component of PAr1 was  $9.0 \times 10^{-10} \text{ Pa}^{-1}$ , and approximately five times smaller than that for UP. Conversely, the intrinsic birefringence for PAr1 was estimated to be 2.5 times smaller than that for PC. This result indicates that reducing stiffness of main chain with flexible junctions and also optical anisotropy are effective in decreasing  $C_R$ . The stress–optical coefficient for the G component of PAr1 was  $3.1 \times 10^{-11} \text{ Pa}^{-1}$ . This value agreed well with that for the polymers containing phenyl rings in their repeating unit. © 1997 Elsevier Science Ltd. All rights reserved.

(Keywords: dynamic birefringence; stress–optical rule; intrinsic birefringence; polyarylate)

### INTRODUCTION

When polymeric materials are deformed, the refractive index tensor becomes anisotropic. Anisotropy of the refractive index can be measured as birefringence, which is strongly related to the stress. Proportionality between the anisotropic parts of the refractive index and the stress tensor is called the stress–optical rule, SOR. This rule holds well for steady-state flows and relaxation processes of polymer melts or concentrated solutions<sup>1,2</sup>. SOR under sinusoidal tensile deformations can be written as follows:

$$O'(\omega) = CE'(\omega) \quad (1) \quad C_R O''(\omega) =$$

where  $O^*(\omega) = O'(\omega) + iO''(\omega)$  and  $E^*(\omega) = E'(\omega) + iE''(\omega)$  are the complex strain–optical ratio and the complex Young’s modulus, respectively. The proportional coefficient,  $C$ , is the stress–optical coefficient, which depends on polymer species but does not depend on the angular frequency,  $\omega$ .

Another well-known relation between the stress and the birefringence is the photoelastic relation (PER) which is applicable to the instantaneous stress and birefringence in the glassy state<sup>3</sup>. In oscillatory elongation, the PER corresponds to

$$O'(\omega) = C_P E'(\omega) \quad (\omega \rightarrow \infty) \quad (3)$$

The photoelastic coefficient,  $C_P$ , is constant for small strains. The PER does not take account of the relaxation phenomena or the effect of the varying frequency in the case of oscillatory deformation.

Because the two coefficients,  $C$  and  $C_P$ , are generally not equal to each other, the birefringence is not proportional to the stress in the glass-to-rubber transition zone of the viscoelastic spectrum. Some modifications of SOR have been proposed to connect the two quantities in these zones<sup>4–6</sup>. Among these modifications, the modified stress–optical rule, MSOR, proposed by Inoue *et al.*<sup>6</sup> succeeded in explaining the complex behaviour of the birefringence relaxation in the glass-to-rubber transition zone. For example, the origin of the complicated frequency dependence of  $O^*(\omega)$ , and the different temperature dependence between  $O^*(\omega)$  and  $E^*(\omega)$  in the transition zone can be explained by MSOR<sup>6</sup>.

According to MSOR, two different mechanisms (denoted by G and R) contribute to the birefringence and the stress around the glass-to-rubber transition zone and the ordinary SOR holds well separately for each component:

$$E^*(\omega) = E_G^*(\omega) + E_R^*(\omega) \quad (4)$$

$$O^*(\omega) = C_G E_G^*(\omega) + C_R E_R^*(\omega) \quad (5)$$

where  $E_i^*(\omega)$  ( $i = G, R$ ) is the complex component function of Young’s modulus for component  $i$ , and  $C_i$  is the stress–optical coefficient for component  $i$ . MSOR

\* To whom correspondence should be addressed

is based on two experimental results; the validity of the ordinary SOR in the rubbery zone and the proportionality of  $O''(\omega)$  to  $E''(\omega)$  in the glassy zone<sup>6</sup>, and therefore  $C_R$  is equal to  $C$  of the SOR. Because equations (4) and (5) are simultaneous equations for  $E_G^*(\omega)$  and  $E_R^*(\omega)$ , the two component functions can be separated quantitatively by reducing the equations.

In previous papers, we have investigated properties of  $E_R^*(\omega)$  and  $E_G^*(\omega)$  and the coefficients  $C_R$  and  $C_G$ <sup>6-12</sup>. The polymers analysed with MSOR are; polystyrene (PS)<sup>6</sup>, poly( $\alpha$ -methyl styrene) (P $\alpha$ MS)<sup>7</sup>, bisphenol A polycarbonate (PC)<sup>8</sup>, polysulfone (PSF)<sup>8</sup>, polyether sulfone (PES)<sup>8</sup>, polyether imide (PEI)<sup>8</sup>, a conventional polyarylate (UP)<sup>9</sup>, polyisoprene (PIP)<sup>10</sup>, and amorphous polyolefins (PEMOMID<sup>11</sup>, PMMTDE<sup>12</sup>, PDOE<sup>12</sup>, PMMCPE<sup>12</sup>, PCHCPE<sup>12</sup>, and PPCPE<sup>12</sup>). Polyisobutylene (PIB)<sup>13</sup>, poly(2-vinyl naphthalene) (PVN)<sup>14</sup>, and poly(alkyl methacrylate)s (PRMA)<sup>15</sup> could not be analysed with MSOR. Osaki *et al.* proposed a theoretical interpretation of MSOR. According to this molecular interpretation, the R component is related to the orientation of the polymer chain while the G component is related to the rotational motion about the main chain axis<sup>22</sup>.

The coefficient,  $C_R$ , is related to the optical-anisotropy of repeating units<sup>16</sup>. Recently, Tanaka and Inoue<sup>17</sup> synthesized a new amorphous polyarylate, PAR1, with low molecular anisotropy. The molecular structure of this polyarylate is shown in Figure 1. The figure also includes the molecular structure of UP and PC. The 2,2'-dicarboxy biphenyl unit in PAR1 effectively compensates for the optical anisotropy of bisphenol A unit. In the present study, we examined the strain-birefringence of PAR1 in order to investigate the relation between molecular structure and the birefringence. It will be shown that PAR1 has a highly flexible main-chain structure which can be attributed to the 'zigzag' structure.

## EXPERIMENTAL

Polyarylate, PAR1, was synthesized with the conventional interfacial emulsion polymerization technique from 4,4'-dioxydiphenyl-2,2'-propane (Bisphenol A, Nakarai Chemical Co.) and 2,2'-dicarboxy biphenyl dichloride (Nippon Johryu Ltd).  $M_w$  and  $M_n$  were determined as  $3.46 \times 10^5$  and  $2.32 \times 10^5$  by gel permeation chromatography with small-angle light scattering. The glass transition temperature measured with differential scanning calorimetry was 162°C. A film was cast from 5wt% dichloromethane solution after filtration through a 0.5 mm pore size membrane filter; the film was then dried in a vacuum dry oven at 165°C for a few days prior to measurements.

The apparatus for dynamic birefringence measurements has been described elsewhere<sup>6</sup>. An optical system was attached to an oscillatory tensile rheometer (Rheology, DVE 3, Kyoto, Japan). A Sénarmont optical system was used to compensate the static birefringence induced by the load maintaining the sample: He-Ne laser, polarizer, quarter-wave plate, analyser, and photodetector were placed on an optical bench. The sample was placed between the polarizer and the quarter-wave plate with their axis at 45° to the strain direction. Available frequency range was 1–130 Hz. The measurements were performed at isothermal conditions at several temperatures.

## RESULTS AND DISCUSSION

### Characteristic behaviour of $E^*(\omega)$ and $O^*(\omega)$

The raw data of the complex Young's modulus,  $E^*(\omega)$ , and the complex strain-optical ratio,  $O^*(\omega)$ , at each temperature are not shown here—only the characteristic behaviour of the two quantities is described. The composite curves for these quantities will be shown later (see Figures 7 and 8). At the highest temperature, 197°C,  $E^*(\omega)$  data corresponded to the onset of the rubbery plateau zone. The ordinary SOR was found to hold well at low frequencies at this temperature. The stress optical coefficient,  $C$ , for PAR1 was estimated as  $9.0 \times 10^{-10} \text{ Pa}^{-1}$ . At lower temperatures, SOR did not hold. However,  $O''(\omega)$  was found to be proportional to  $E''(\omega)$  over the temperature range 162–157°C. The proportional coefficient,  $C_G$ , was  $3.1 \times 10^{-11} \text{ Pa}^{-1}$ .

$C_G$  and  $C_R (=C)$  are summarized in Table 1 with the values for PC<sup>8</sup>, and UP<sup>9</sup>. The  $C_R$  value for PAR1 is about eight times smaller than that for UP. The  $C_G$  values of the three polymers are almost the same and the similar values were found for other polymers containing phenyl groups<sup>8</sup>.

### Analysis with modified stress-optical rule

With the determined  $C_R$  and  $C_G$ , equations (3) and (4) were solved for  $E_G^*(\omega)$  and  $E_R^*(\omega)$  at each temperature, considering the possibility of different temperature dependence between  $E_G^*(\omega)$  and  $E_R^*(\omega)$ . The method of reduced variables<sup>18</sup> was then used individually for the two components to construct the respective composite curves.

Figure 2 shows the resulting composite curves of  $E_G^*(\omega)$  and  $E_R^*(\omega)$  for PAR1. The data for the R

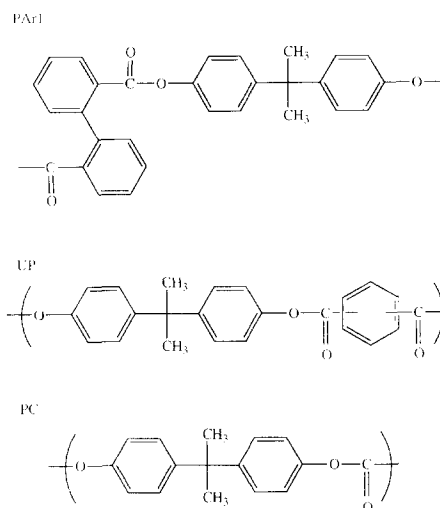


Figure 1 Molecular structure of the polyarylate, PAR1, a conventional polyarylate, UP, and bisphenol A polycarbonate, PC

Table 1 Summary of values for the various characteristic moduli and the stress-optical coefficients

Polymer	$E_R'(\infty)$ (MPa)	$E_G'(\infty)$ (MPa)	$\gamma^b$	$C_R$ (Br) <sup>a</sup>	$C_G$ (Br)	$C_p$ (Br)	$\Delta n^0$
PAR1	53	1150	4.7	900	31	72	0.0080
UP	27	1120	11	6800	38	202	0.031
PC	26	1500	11	4700	35	116	0.020

<sup>a</sup> Brewsters =  $10^{-12} \text{ Pa}^{-1}$

<sup>b</sup> See the text for definition

component at the two lowest temperatures are eliminated: at these temperatures the shift factor cannot be determined because  $E'_R(\omega)$  is a constant independent of frequency and temperature,  $5.1 \times 10^7$  Pa, and  $E''_R(\omega)$  is close to 0 with scattering of data. The R and G components of PAR1 will be discussed in detail in the following sections compared with those of PC and UP.

Figure 3 illustrates the shift factors used in the construction of the composite curves for the component functions. Although temperature dependence of the two shift factors is fairly close, careful comparison reveals that the shift factor for the G component shows slightly stronger temperature dependence than that for the R component. The stronger temperature dependence for the G component is widely observed in our previous studies<sup>6-12</sup>.

#### The R component

Figure 4 shows the R component functions for PAR1, PC<sup>8</sup>, and UP<sup>9</sup>. Here, the reference temperature,  $T_r$ , is 182°C for PAR1, 156°C for PC, and 211°C for UP. These temperatures were chosen so that  $E''_G(\omega)$  of each polymer came close to  $10^{-8}$  Pa<sup>-1</sup> at  $\omega = 10$  s<sup>-1</sup>.

The R component of PAR1 appears to differ from those of the other two polymers in shape. The difference of the R components can be represented by the difference of two characteristic moduli, the limiting value of  $E'_R(\omega)$  at high frequencies,  $E'_R(\infty)$ , and the rubbery plateau modulus,  $E_N$ .  $E'_R(\infty)$  of PAR1 is about two times higher compared with the two polymers, and this value is the highest value among the polymers examined previously<sup>6-12</sup>. Conversely, the  $E_N$  value of PAR1 is much smaller than those of UP and PC. This low value for PAR1 contrasts with the high  $E_N$  values observed for PC, UP, PES, and PSF, which appears to be a fairly common feature for the amorphous polymers containing benzene rings in the main chain<sup>8</sup>.

Because of the large difference between  $E'_R(\infty)$  and  $E_N$ ,  $E''_R(\omega)$  of PAR1 is similar to those of polystyrene<sup>6</sup> and polyisoprene<sup>10</sup>: the Rouse-like behaviour,  $E''_R(\omega) \propto \omega^{1/2}$ , is clearly observed in a wide range of frequency,  $\log(\omega/\text{s}^{-1}) = -3$  to 1. According to the beads-spring model,  $E'_R(\infty)$  can be related to the molecular weight of the submolecule or the Rouse segment as  $M_S = E'_R(\infty)/3\rho RT$ , where  $\rho$  is density, and  $R$  the gas constant.  $M_S$  of PAR1 is calculated as 280, which is approximately 0.7 times of the repeating unit of PAR1. This result suggests that the main chain of PAR1 is highly flexible. Here, we note a possibility of high flexibility of PAR1. The static flexibility can be described by the characteristic ratio,  $C_\infty = \langle R_g^2 \rangle / \langle R_g^2 \rangle_0$ , where  $\langle R_g^2 \rangle$  and  $\langle R_g^2 \rangle_0$  are the mean-square radius of gyration for unperturbed condition and for the freely jointed chains, respectively. Although  $C_\infty$  of PAR1 has not been measured, it may be estimated according to the free rotating chain model;  $C_\infty$  is related to the coherent bond angle of the main chain,  $\xi$ , as  $C_\infty = (1 + \cos \xi)/(1 - \cos \xi)$ . Therefore, the large bond angle due to the zigzag structure of 2,2'-dicarboxy phenyl unit is probably effective in decreasing  $C_\infty$  even if the rotational hindrance exists. A preliminary molecular simulation using RIS model in Biosystem's Polymer program gave  $C_\infty = 2.4$  for PAR1 and  $C_\infty = 3.5$  for PC. These results also support our conclusion.

The frequencies where  $E''_R(\omega)$  of each polymer indicates a maximum in Figure 4 depends on polymer

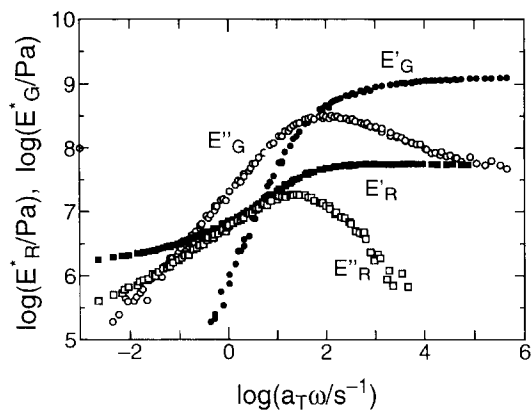


Figure 2 The G and R component functions (see text) for PAR1. Reference temperature is 177°C

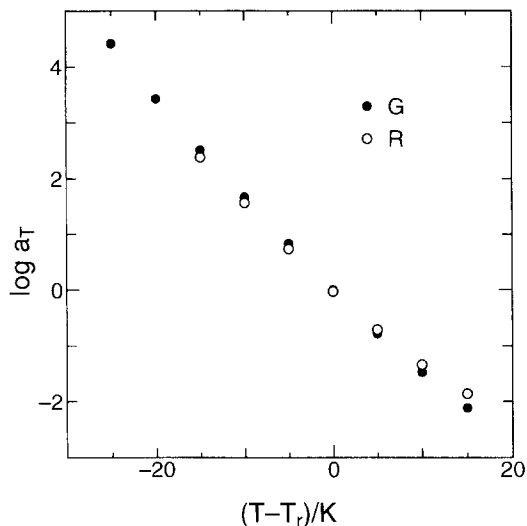


Figure 3 Temperature dependence of the shift factors for the G and R components (see text). Reference temperature is 177°C

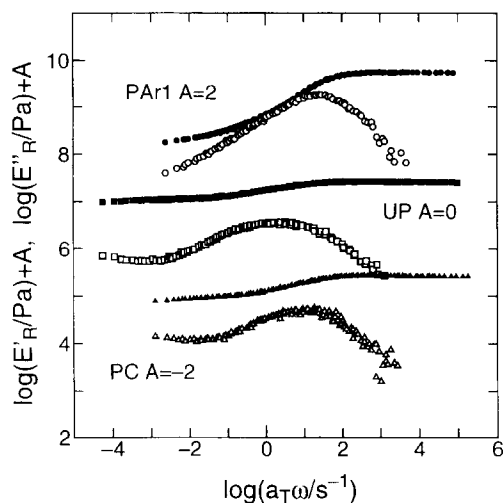


Figure 4 Comparison of the R components functions for PAR1, PC, and UP

species. This derives from the difference of a relative distance between characteristic relaxation times of the G and R components at the reference temperature. In order to characterize the relative position of the two

components, we define a ratio,  $\gamma$ , of two frequencies where  $E''_R(\omega)$  and  $E''_G(\omega)$ , respectively, have a maximum at reference temperature. Note that the value of  $\gamma$  depends slightly on temperature because the G and R components have different temperature dependence, as mentioned previously. Nevertheless, Table 1 suggests the correlation between  $\gamma$  and ratio  $E'_R(\infty)/E'_G(\infty)$ . The frequency where  $E''_R(\omega)$  has a maximum corresponds to the shortest relaxation time for the Rouse segment while the frequency for maximum for  $E''_G(\omega)$  may relate to the most probable relaxation time for a unit of motion which controls the relaxation of the G component. Therefore,  $\gamma$  may correspond to difference of the relative size between the basic relaxation units for the R and the G components. The smaller value of  $\gamma$  for PAr1 is consistent with the highly flexible main-chain structure and the small segment size.

#### The G component

Figure 5 shows the G component functions for PAr1, PC<sup>8</sup>, and UP<sup>9</sup>;  $T_r$  values are the same as in Figure 4. At first sight,  $E'_G(\omega)$  for the three polymers are similar to each other. This result contrasts with the difference found in the R component. A more sensitive and clearer way of comparing the G component is to calculate  $\tan \delta$  of  $E'_G(\omega)$ ,  $\tan \delta_G$ . The resulting  $\tan \delta_G$  of the three polymers are shown in Figure 6;  $\tan \delta_G$  for each polymer is shifted vertically to avoid overlap of data. In the frequency region of  $\omega > 10 \text{ s}^{-1}$ ,  $\tan \delta_G$  for PAr1 agrees well with that for PC. In  $\omega < 10 \text{ s}^{-1}$ , the slope of  $\tan \delta_G$  for PAr1 is steeper than that of PC and it is close to  $-1$ . Conversely,  $\tan \delta_G$  for UP is gradual over the whole frequency range. This feature of UP may be due to the heterogeneity of the main chain structure of UP because UP is synthesized from 1:1 mixture of isophthalic and terephthalic acids. Local motions of UP would not be uniform and this would cause a wider distribution of the relaxation time.

The limiting values of  $E'_G(\omega)$  at high frequencies,  $E'_G(\infty)$ , are shown in Table 1. It appears likely that  $E'_G(\infty)$  of PAr1 and UP are slightly smaller than PC.  $E'_G(\infty)$  would relate to the origin of the stress in the glassy state. It may represent a property of the conformer proposed by Matsuoka<sup>19</sup>.

#### Stress-optical coefficients

The value of  $C_R$  for PAr1 is about five times smaller than for PC. This result indicates that the segment of PAr1 has the smaller optical anisotropy.

A quantity characterizing the orientational birefringence of polymers is the intrinsic birefringence,  $\Delta n^0$ , which is defined as follows<sup>20</sup>

$$\Delta n = \Delta n^0 P \quad (6)$$

Here  $P$  is the orientation factor

$$P = (3\langle \cos^2 \theta \rangle - 1)/2 \quad (7)$$

$\theta$  is the angle between the direction of stretch and the segment.  $\Delta n^0$  may be called the maximum birefringence because the perfect orientation corresponds to  $P = 1$ . According to the affine or quasi-affine deformation models,  $P$  can be related to the stretch ratio,  $\lambda$ , in infinitesimal strain.

$$P = (\lambda^2 - 1/\lambda)/5 = 3\varepsilon/5 \quad (8)$$

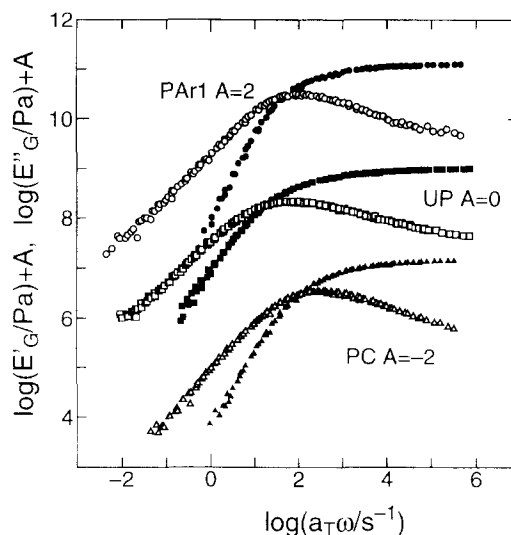


Figure 5 Comparison of the G components functions for PAr1, UP and PC

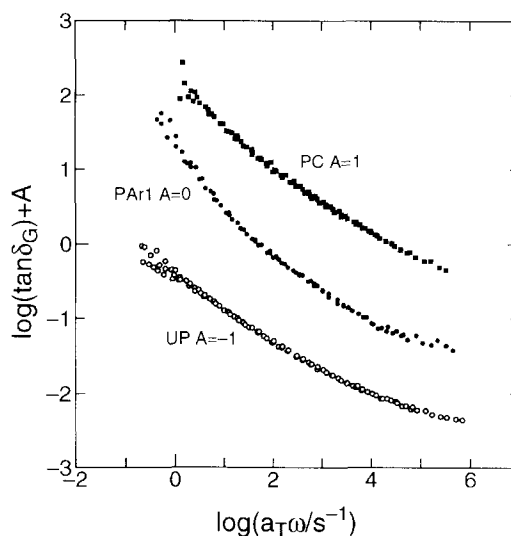


Figure 6 Comparison of  $\tan \delta$  for the G component for PAr1, UP and PC

Using equation (8),  $\Delta n^0$  can be related to the limiting value of  $O'_R(\omega)$  ( $\equiv \Delta n/\varepsilon$ ) at high frequencies provided that the R component is originated by the segment orientation.

$$\Delta n^0 = 5O'_R(\infty)/3 = 5C_R E'_R(\infty)/3 \quad (9)$$

The value of  $\Delta n^0$  for PAr1 is 0.008, which is about 2.5 times smaller than that for PC. Thus, the intrinsic birefringence of PAr1 is not so small. This derives from relatively large  $E'_R(\infty)$ , that is, the flexible chain structure due to the 2,2'-dicarboxy biphenyl unit.

Through the Lorentz-Lorenz equation,  $\Delta n^0$  can be related to the anisotropy of the segment<sup>20</sup>

$$\Delta n^0 = (2\pi/9)\{(n^2 + 2)^2/n\}(\rho N_a/M_S)\Delta\alpha \quad (10)$$

where  $n$  is the refractive index and  $\Delta\alpha$  is the difference between the principal values of the polarizability tensor of the segment in the parallel and perpendicular directions of the chain axis;  $\rho$  and  $N_a$  are the density and the Avogadro's number, respectively. For polymers composed of simple repeating units, such as vinyl polymers,

$\Delta\alpha$  may be approximately related to the anisotropy of the repeating unit<sup>21</sup>,  $\Delta\alpha^0$

$$\Delta\alpha = \Delta\alpha^0 M_S/M_0 \quad (11)$$

where  $M_0$  is the molecular weight of the repeating units. This relation may be explained by considering that the maximum orientation ( $P = 1$ ) is defined as the fully extended state where the axis of chain orients along the stretch direction with all-*trans* conformation. However, for PAR1, the structure of repeating unit is complex and the size of the repeating unit of PAR1 is larger than the segment size estimated from  $E_R(\infty)$ . Therefore,  $\Delta n^0$  of PAR1 corresponds to the anisotropy of the repeating unit at extended state.

In previous studies, the  $C_G$  value of polymers with a high benzene ring content was found to be relatively constant,  $3 \times 10^{-12} \text{ Pa}^{-1}$ : this is the case for PAR1. The 2,2'-dicarboxy biphenyl unit is effective to reduce  $C_R$ , but it does not affect  $C_G$  values. This result can be explained by the theoretical interpretation of MSOR, in which  $C_G$  is related to the axial symmetry of optical anisotropy of the segment or the repeating unit about the main-chain direction<sup>22</sup>.

#### Comparison of master curves

In order to compare  $E^*(\omega)$  and  $O^*(\omega)$  over a wide frequency range, the construction of master curves by the method of reduced variables is useful if they are thermo-rheologically simple. However, this is not the case for  $E^*(\omega)$  and  $O^*(\omega)$  around the glass transition zone because the two component functions show different temperature dependence. Therefore, we cannot directly apply the method of reduced variables for these quantities. The best way to obtain the master curves of  $E^*(\omega)$  and  $O^*(\omega)$  is to reproduce them using the modified stress-optical rule from the master curves of two component functions which are thermo-rheologically simple.

Figure 7 shows  $E^*(\omega)$  of the two polyarylates and PC obtained by the above method. The characteristic behaviour of  $E^*(\omega)$  for the three polymers is similar and typical in the vicinity of the glass-to-rubber transition zone. One major difference of PAR1 from the other polymers is height of  $E_N$ , as seen before. Because of this difference,  $\tan \delta \equiv E''(\omega)/E'(\omega)$  of PAR1 in the transition zone is larger compared with the two polymers. For UP, the broader frequency dependence of the  $G$  component also reduces  $\tan \delta$  in this zone.

Figure 8 indicates  $O^*(\omega)$  obtained in the same way as  $E^*(\omega)$ .  $O^*(\omega)$  of the three polymers is positive in the whole of the measured frequency range.  $O'(\omega)$  of UP and PC varies only about three times in the measured frequency region while  $O'(\omega)$  of PAR1 decreases almost 50 times with decreasing frequency. In the rubbery plateau zone, the  $O'(\omega)$  of PAR1 is about 20 times smaller than that of PC. This derives from lower  $C_R$  and lower  $E_N$  of PAR1. Conversely, the difference of  $O'(\omega)$  between PAR1 and UP or PC in the glassy zone is about two times: the birefringence of PAR1 in the glassy zone is not reduced as much as the rubbery zone. One reason for this result is the high  $E_R(\infty)$  of PAR1. In addition, there is the nearly constant contribution of the  $G$  component to birefringence in the glassy zone because  $C_G E_G(\infty)$  of the three polymers does not vary as much (0.03–0.05). For PAR1, the contribution of the  $G$  component to birefringence in the glassy zone is comparable to that of the  $R$

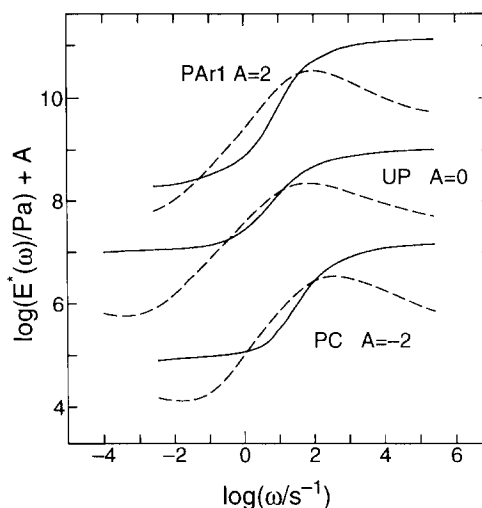


Figure 7 Composite curves of the complex Young's modulus for PAR1, UP, and PC. Continuous lines show  $E'(\omega)$  and broken lines show  $E''(\omega)$ . Each curve was constructed from the composite curves of the two components in Figures 4 and 5 through the modified stress-optical rule. See the text for details

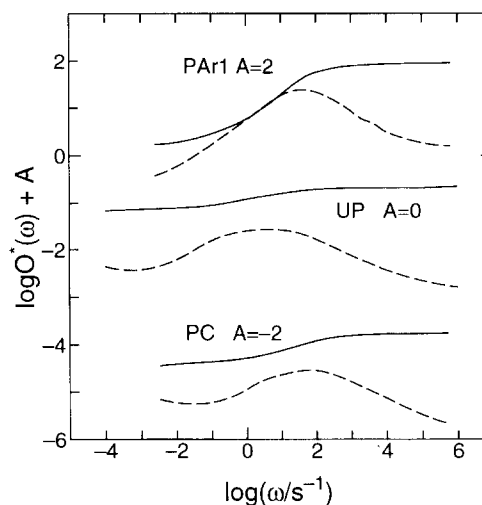


Figure 8 Composite curves of the strain-optical ratio for PAR1, UP, and PC. Continuous lines show  $O'(\omega)$  and broken lines show  $O''(\omega)$ . Each curve was constructed by the same scheme as Figure 7

component. However, for PC and UP the contribution of the  $G$  component to the birefringence in the glassy zone is relatively small.

#### CONCLUSION

Dynamic birefringence and viscoelasticity of PAR1 with a low optical anisotropy were studied in the vicinity of the glass-to-rubber transition zone. The modified stress-optical rule was applicable to PAR1 and the  $R$  and  $G$  component functions were determined. The  $R$  component for PAR1 has the lower rubbery plateau modulus,  $E_N$ , and higher  $E_R(\infty)$  compared with UP and PC. For this reason, the  $R$  component of PAR1 is similar to that of polystyrene and polyisoprene instead of UP and PC, and the Rouse-like behaviour is observed over a wide frequency range. The high  $E_R(\infty)$  value suggests that the main chain of PAR1 is fairly flexible. This flexible chain structure could be attributed to a zigzag structure brought about by the 2,2'-dicarboxy biphenyl unit. The

$E_N$  value of PAr1 was about four times lower than those for UP and PC, contrasting with the high  $E_N$  values commonly observed for engineering plastics. The G component of PAr1 showed a similar frequency dependence to that of PC, except low frequencies, while that for UP showed a slightly broader frequency dependence. PAr1 has a smaller  $C_R$  value compared with PC and UP, while  $C_G$  value of the three polymers is nearly constant. The smaller  $C_R$  value for PAr1 could be attributed to the small optical anisotropy of repeating unit and to the flexible chain structure.

#### ACKNOWLEDGEMENT

This study was supported by a Grant-in-Aid for Scientific Research (07455382) of the Ministry of Culture, Science, and Education of Japan.

#### REFERENCES

- 1 Wales, J. L. S. 'The Application of Flow Birefringence to Rheological Studies of Polymer Melts', Delft University Press, Rotterdam, 1976
- 2 Janeschitz-Kriegl, H. 'Polymer Melt Rheology and Flow Birefringence', Springer-Verlag: Berlin, 1983
- 3 Brewster, D. *Trans. Roy. Soc. (London)* 1816, **106**, 156
- 4 Priss, L. S., Vishnyakovm, I. I. and Pavlova, I. P. *Int. J. Polym. Mater.* 1980, **8**, 85

- 5 Read, B. E. *Polym. Eng. Sci.* 1983, **23**, 835
- 6 Inoue, T., Okamoto, H. and Osaki, K. *Macromolecules* 1991, **24**, 5670
- 7 Inoue, T., Hwang, E. J. and Osaki, K. *J. Rheology* 1992, **36**, 1737
- 8 Hwang, E. J., Inoue, T. and Osaki, K. *Polym. Eng. Sci.* 1994, **34**, 135
- 9 Hwang, E. J., Inoue, T. and Osaki, K. *Polymer (Korea)* 1993, **17**, 249 (in Korean)
- 10 Okamoto, H., Inoue, T. and Osaki, K. *J. Polym. Sci. Polym. Phys. Ed.* 1995, **33**, 417
- 11 Inoue, T., Takiguchi, O., Osaki, K., Kohara, T. and Natsuume, T. *Polym. J.* 1994, **26**, 133
- 12 Inoue, T., Okamoto, H., Osaki, K., Kohara, T. and Natsuume, T. *Polym. J.* 1995, **9**, 943
- 13 Okamoto, H., Inoue, T. and Osaki, K. *J. Polym. Sci. Polym. Phys. Ed.* 1995, **33**, 1409
- 14 Hwang, E. J., Inoue, T., Osaki, K. and Takano, A. *Nihon Reoroji Gakkaishi* 1994, **22**, 129
- 15 Takiguchi, O., Inoue, T., Osaki, K. and Takano, A. *Nihon Reoroji Gakkaishi* 1995, **23**, 13.
- 16 Riande, E. and Saiz, E. 'Dipole Moments and Birefringence of Polymers', Prentice Hall, Englewood Cliffs, 1994
- 17 Tanaka, T. and Inoue, T. *J. Non-Cryst. Solids* 1991, **131-133** (pt. 2), 781
- 18 Ferry, J. D. 'Viscoelastic Properties of Polymers', 3rd edn, Wiley, New York, 1980, Chapter 11, pp. 264-320
- 19 Matsuoka, S. 'Relaxation Phenomena in Polymers', Hanser Publishers, New York, 1992
- 20 Ward, I. M. 'Structures and Properties of Oriented Polymers', Applied Science Publishers, New York, 1992
- 21 Spector, K. S. and Stein, R. S. *Macromolecules* 1991, **24**, 2083
- 22 Osaki, K., Okamoto, O., Inoue, T. and Hwang, E. J. *Macromolecules* 1995, **28**, 3625